Available online at www.sciencedirect.com
SCIENCE DIRECT®
Deep-Sea Research I 52 (2005) 2376–2389
DEEP-SEA RESEARCH PART I
www.elsevier.com/locate/dsr

Instruments and Methods

Development and deployment of a precision underwater positioning system for in situ laser Raman spectroscopy in the deep ocean

Sheri N. White[a,*], William Kirkwood[b], Alana Sherman[b], Mark Brown[b], Richard Henthorn[b], Karen Salamy[b], Peter Walz[b], Edward T. Peltzer[b], Peter G. Brewer[b]

[a]*Department of Applied Ocean Physics & Engineering, Woods Hole Oceanographic Institution, Woods Hole, MA 02543, USA*
[b]*Research & Development, Monterey Bay Aquarium Research Institute, 7700 Sandholdt Road, Moss Landing, CA 95039, USA*

Received 5 April 2005; received in revised form 31 August 2005; accepted 9 September 2005

Abstract

The field of ocean geochemistry has recently been expanded to include in situ laser Raman spectroscopic measurements in the deep ocean. While this technique has proved to be successful for transparent targets, such as fluids and gases, difficulty exists in using deep submergence vehicle manipulators to position and control the very small laser spot with respect to opaque samples of interest, such as many rocks, minerals, bacterial mats, and seafloor gas hydrates. We have developed, tested, and successfully deployed by remotely operated vehicle (ROV) a precision underwater positioner (PUP) which provides the stability and precision movement required to perform spectroscopic measurements using the Deep Ocean Raman In situ Spectrometer (DORISS) instrument on opaque targets in the deep ocean for geochemical research. The positioner is also adaptable to other sensors, such as electrodes, which require precise control and positioning on the seafloor. PUP is capable of translating the DORISS optical head with a precision of 0.1 mm in three dimensions over a range of at least 15 cm, at depths up to 4000 m, and under the normal range of oceanic conditions (T, P, current velocity). The positioner is controlled, and spectra are obtained, in real time via Ethernet by scientists aboard the surface vessel. This capability has allowed us to acquire high quality Raman spectra of targets such as rocks, shells, and gas hydrates on the seafloor, including the ability to scan the laser spot across a rock surface in sub-millimeter increments to identify the constituent mineral grains. These developments have greatly enhanced the ability to obtain in situ Raman spectra on the seafloor from an enormous range of specimens.
© 2005 Elsevier Ltd. All rights reserved.

Keywords: Optical instruments; Underwater vehicles; Oceanographic equipment; Raman spectroscopy; Motion control

1. Introduction

Early geochemical studies of the ocean floor relied upon dredges deployed from surface ships to pull up seafloor material for laboratory-based analyses. As technology progressed, manned and

*Corresponding author. Tel.: +1 508 289 3740; fax: +1 508 457 2006.
E-mail address: swhite@whoi.edu (S.N. White).

0967-0637/$ - see front matter © 2005 Elsevier Ltd. All rights reserved.
doi:10.1016/j.dsr.2005.09.002

unmanned submersibles have allowed scientists to actually view the ocean floor, to observe the changes from sedimented abyssal plains to rocky mid-ocean ridges (e.g., Ballard et al., 1975), and to visually select material for analysis. Today, imaging systems such as high definition video provide the most detailed images to date of the ocean floor with its enormous range of biological communities and geochemical sites, such as high-temperature hydrothermal vents and ice-like hydrate exposures.

Visual identification can provide only so much information. For example, a white solid object on the seafloor may be aragonite, calcite, barite, or anhydrite; and a hydrate exposure may have a wide range of chemical constituents, yet simply appear ice-like to the viewer. The ability to determine chemical structure, and to observe chemical processes in situ would be of great importance to users of deep submergence vehicles and platforms. Laser Raman spectroscopy is capable of performing these in situ measurements on solids, liquids and gases in the deep ocean (Brewer et al., 2004; Pasteris et al., 2004).

One challenge of deep-sea laser Raman spectroscopy is positioning the laser spot with the precision required to obtain spectra from opaque targets. To date, laser Raman spectroscopy has been limited to transparent objects because of the small focal depth (i.e., 0.15–3.0 mm) sampling optics, and the difficulty of precise positioning of the focal spot by a deep submergence vehicle. Remotely operated vehicle (ROV) robotic arms are sometimes prone to jitter, and ocean forcing can cause vibrations of the ROV itself. These can result in the inability to properly position the laser spot, and the inability to maintain the position for the required data acquisition time. Solution of these problems would therefore greatly extend the generality of this technique, and its usefulness for ocean research. We have therefore developed a precision positioning system deployable by ROV for use with a deep-ocean laser Raman spectrometer. In this paper, we present the development of the precision underwater positioner (PUP) for the acquisition of high quality Raman spectra of opaque targets on the seafloor. It should be noted that although PUP was designed for use with the Deep Ocean Raman In situ Spectrometer (DORISS) instrument (Brewer et al., 2004), it is a stand-alone system that can be used with other sensors that have similar positioning requirements.

2. Background

Laser Raman spectroscopy is a type of vibrational spectroscopy in which a monochromatic laser is used to excite a target and the inelastically backscattered light is measured (e.g., Nakamoto, 1997). The peaks observed in the Raman spectrum are due to the vibrational modes of the target molecule; thus information about both chemical composition and structure is obtained. Laser Raman spectroscopy is rapid, non-destructive, and can be performed in situ, making it a powerful tool for performing geochemical analyses in the ocean. In addition, it can be used to analyze solid, liquid or gaseous targets.

Brewer et al. (2004) developed and successfully deployed a sea-going laser Raman spectrometer (DORISS). DORISS is based on a laboratory model Kaiser HoloSpec f/1.8i spectrometer (Owen et al., 1998) with a holographic transmissive grating and a 2048×512 CCD camera by Andor Technology. For deployment in the deep ocean (up to 4000 m depth) the components have been divided into three pressure housings. The housings containing the spectrometer, laser, and single-board computer are mounted in the ROV toolsled (Fig. 1). The probe head is contained in a 35.5-cm-long, 14-cm-diameter titanium housing. It is connected to the laser and spectrometer via pressure-tolerant fiber optic cables. The probe head is carried on the front of the ROV

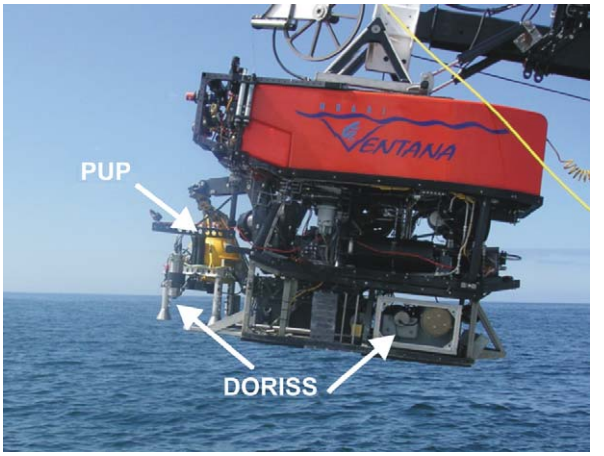

Fig. 1. DORISS and PUP being deployed on the ROV *Ventana*. The DORISS electronics and spectrometer housings are mounted in a drawer in the back of the ROV toolsled. The DORISS probe head and the PUP are carried on the front porch and secured by the ROV manipulator.

and can be positioned at a target of interest with the ROV manipulator (Fig. 2). DORISS has been deployed over a dozen times in Monterey Bay and the Gulf of California. It has been successfully used to perform gas dissolution experiments (White et al., in press), to analyze gas hydrates (Hester et al., in press), and to analyze natural gas venting from the seafloor (White et al., 2003).

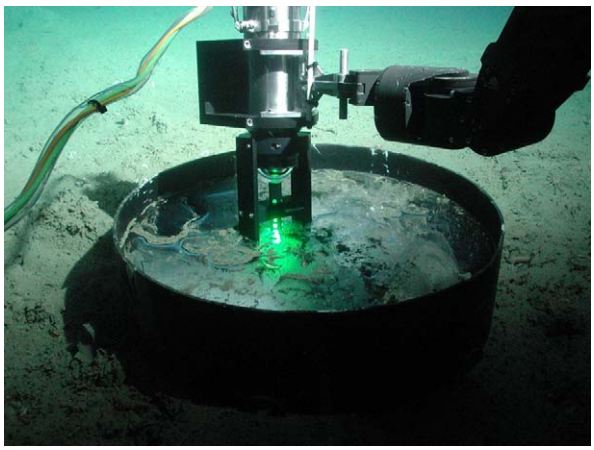

Fig. 2. The DORISS probe head is positioned over a pool of liquid on the seafloor (3607 m depth) by the ROV manipulator. The fiber optic cables connecting the probe head to the DORISS electronics and spectrometer housings can be seen on the left.

3. System specification

3.1. Science drivers

The DORISS instrument has a very small focal volume—the laser spot size is on the order of tens of microns, and the depth of focus is as small as ~0.15 mm in water (Fig. 3). When analyzing transparent targets, the focal point is positioned inside the volume of the target. However, when analyzing an opaque target, the focal point must be positioned exactly at the surface of the material. This requires the ability to position the target with respect to the probe head with a precision of ~0.1 mm in the direction normal to the surface. Using a larger depth-of-focus optic would ease the positioning requirements, but would decrease the power density, thus decreasing the Raman signal from the target.

The two approaches to precision positioning are: (1) present the target to a stationary probe head, or (2) present the probe head to the stationary target. The key advantage of DORISS over other techniques is the ability to non-destructively analyze a specimen in situ without any sample preparation or any sample alteration caused by sample collection, recovery, or storage. In order to maintain the experimental flexibility that DORISS provides, positioning the probe head is favored. During initial

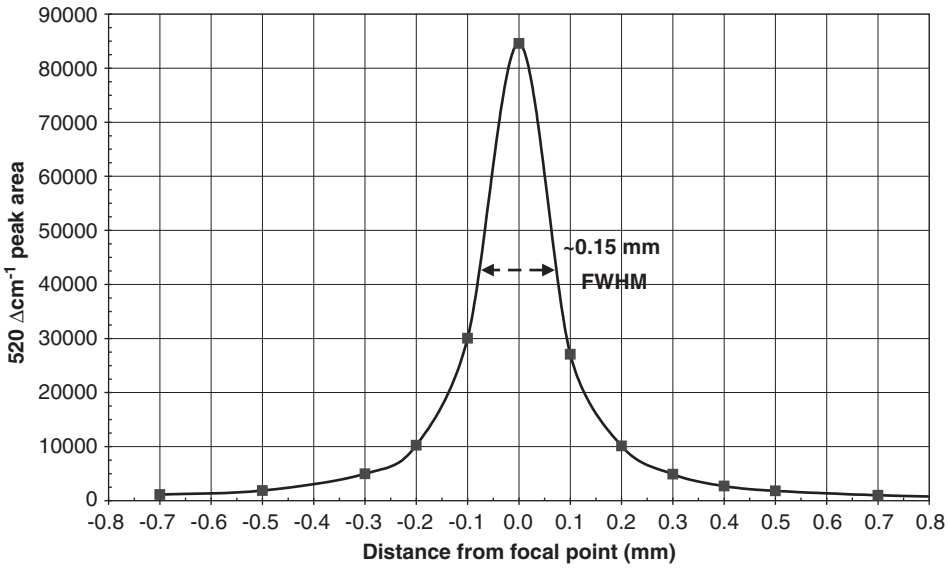

Fig. 3. The depth of focus of the immersion optic is determined by collecting spectra from a polished silicon wafer. As the optic is moved in 0.1 mm increments, the intensity of the characteristic 520 $\Delta\,cm^{-1}$ peak of silicon is measured. The full width at half maximum (FWHM) is the depth of focus (~0.15 mm for this optic).

deployments of the DORISS instrument, the probe head was positioned with the ROV manipulator. This method was successful for analyzing transparent pools of liquid CO_2 on the seafloor (Fig. 2) and semitransparent samples of calcite. However, it was quite difficult to obtain spectra from opaque rock samples in this manner.

The PUP was developed to provide the stability and precision positioning needed to collect quality Raman spectra of opaque targets on the seafloor (e.g., carbonates, hydrothermal minerals and bacterial mats). Ideally, the PUP would be generic enough to support the DORISS probe head in various configurations, and would be able to serve the needs of other types of instrumentation that may require precision positioning (e.g., deep sea microscopy).

3.2. Design concept

Several concepts were considered to meet the functional requirements (listed in the Appendix A) including a 3 degrees of freedom (DOF) Cartesian system (i.e., *X*-*Y*-*Z*) and a 6 DOF Stewart platform (i.e., hexapod). The *X*-*Y*-*Z* and hexapod platforms did not provide adequate flexibility for DORISS operations, and could not easily meet the size and weight requirements. The concept selected was a 5 DOF system (Fig. 4A). The axes of motion are *Z* (up-and-down), *R* (in-and-out), and θ (rotation about the *Z*-axis). A pan & tilt device at the sensor head provides the remaining 2 DOF. A tripod platform is used for stability with adjustable legs to accommodate various seafloor topologies. By off-loading PUP onto the seafloor, it is decoupled from any ROV motion. A small web camera, light, and lasers are mounted on the sensor head to aid in positioning. The two lasers are positioned to cross at the focal point of the DORISS laser beam. The camera allows the user to observe the locations of the DORISS laser and the positioning lasers on the target. The laser spots move closer to one another as the DORISS focal spot approaches the surface of the target.

Because of time and resource limitations, the phase I prototype consists of 3-DOF (*Z*, *R*, and θ), with rigid legs, and a camera, light and lasers (Fig. 4B). Additional axes and features will be added as time and resources permit.

4. System build

A system block diagram for the DORISS/PUP system is shown in Fig. 5. PUP consists of actuators, a camera, light, lasers, and electronics (e.g., servos, motion controllers, Ethernet hub and video server) in a single off-loadable unit. As noted above, the DORISS electronics and spectrometer housing are mounted in the ROV toolsled. An additional housing, the vehicle interface can (VIC), is also mounted in the toolsled and provides a single power and communications interface to the ROV for both DORISS and PUP. Note that DORISS and PUP can each be used individually on the ROV without the VIC housing. The ROV provides power (ROV *Tiburon*: 240 VDC; ROV *Ventana*: 110 VAC) and

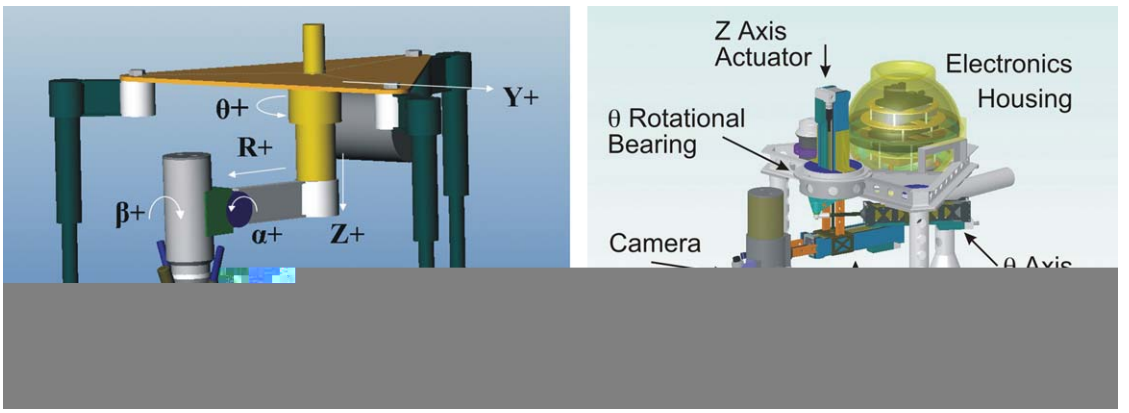

Fig. 4. (A) The design concept for the precision underwater positioner (PUP) calls for a tripod platform with 5 degrees of motion: *Z* (up-and-down), *R* (in-and-out), θ (rotation about the *Z*-axis), and pan and tilt at the probe head (alpha and beta in the figure). Two lasers and a camera are shown mounted to the sensor head to aid in positioning. (B) The prototype design consists of 3 degrees of motion all driven by linear actuators, rigid legs, a camera, and lasers.

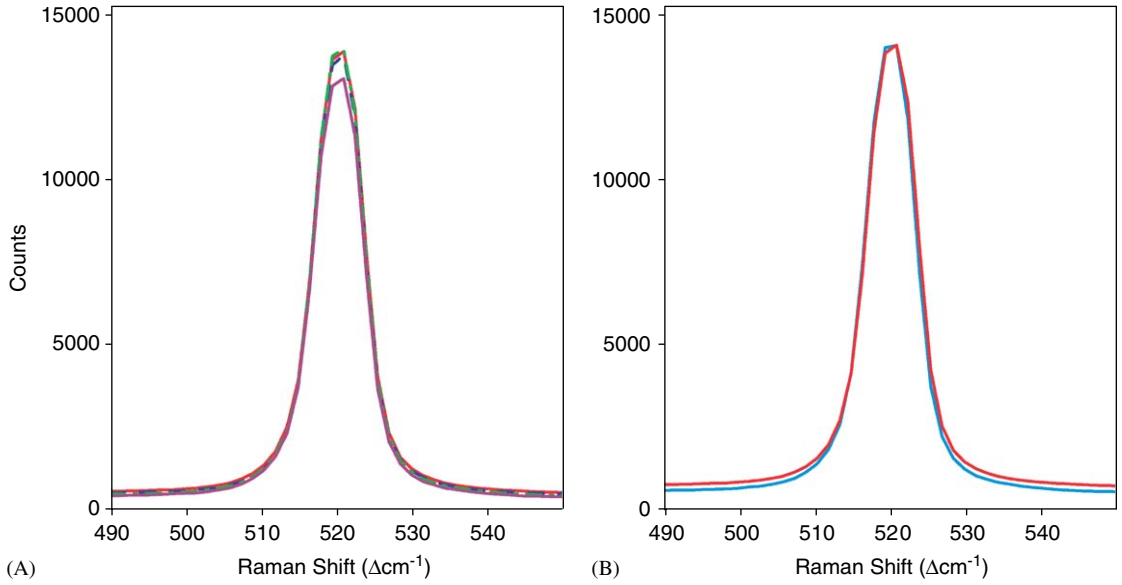

Fig. 12. Raman spectra of a polished silicon wafer obtained using DORISS and PUP. The red line is the initial spectrum collected at position $Z = 100.0$ mm, $R = 100.0$ mm, $\theta = 30.0°$. In plot A, the blue dashed-dotted line was collected after the Z-axis was retracted then returned to the same position. The green dashed line was collected after both the Z and R axes were retracted then returned to the same position. The purple line was collected after all three axes (Z, R, and θ) were retracted then returned to the same position. In plot B, the blue line was collected after all three axes had been moved back and forth throughout their full ranges of motion. The position during the collection of this spectrum was ($Z = 99.9$ mm, $R = 100.0$ mm, $\theta = 29.8°$).

Z-axis. Since a 1.0×1.0 mm mask was used in the horizontal plane, we can only state that the R and θ axes are repeatable to within ~1.0 mm.

6. Field results

PUP and DORISS have been deployed a number of times in the deep ocean for testing, and exploratory measurements. Field deployments in Monterey Bay to depths as great as 1022 m provided the opportunity to test all of the components of the PUP system, and to solve minor problems related to the effects of the cold, high-pressure deep-sea environment. Additionally, Raman spectra were acquired with the DORISS instrument which proved the necessity and effectiveness of PUP.

Known samples of marble, granite and other rocks were carried to the seafloor for Raman analysis. With PUP, we were able to successfully collect spectra from these solid, opaque targets, and we collected spectra along profiles and grid patterns in increments as fine as 0.1 mm. Fig. 13 compares spectra from a slab of marble obtained on the seafloor and in the lab using PUP to position the DORISS probe head. The seafloor spectrum is slightly noisier than the lab spectrum, but compares quite favorably. The O–H stretching bands of water present in the seafloor spectrum are due to the seawater in the optical path.

A slab of granite was analyzed on the seafloor to test the ability of DORISS/PUP to scan over a heterogeneous sample and to obtain information about the bulk composition (Fig. 14). This type of point-counting technique is described by Haskin et al. (1997). We conducted two grid scans over the granite sample. The first consisted of 20 points in a 5×4 grid of 0.1 mm increments. This grid mapped out a grain of the mineral albite bounded on one side by microcline, and on one corner by quartz (Fig. 15). Most of the spectra indicated a single mineral at each point. One point on the albite-quartz boundary contained peaks from both minerals. A second grid of 5 mm increments was used to collect data to determine information about the bulk composition of the rock. Because of time limitations, spectra were collected from only a 3×3 grid (with points numbered 1–9). While the number of data points is too low for a statistically significant analysis, the data do show the expected trends. The minerals identified are listed in Table 1, and a few representative spectra are shown in Fig. 16. In most cases, the spectra at each point indicated a single

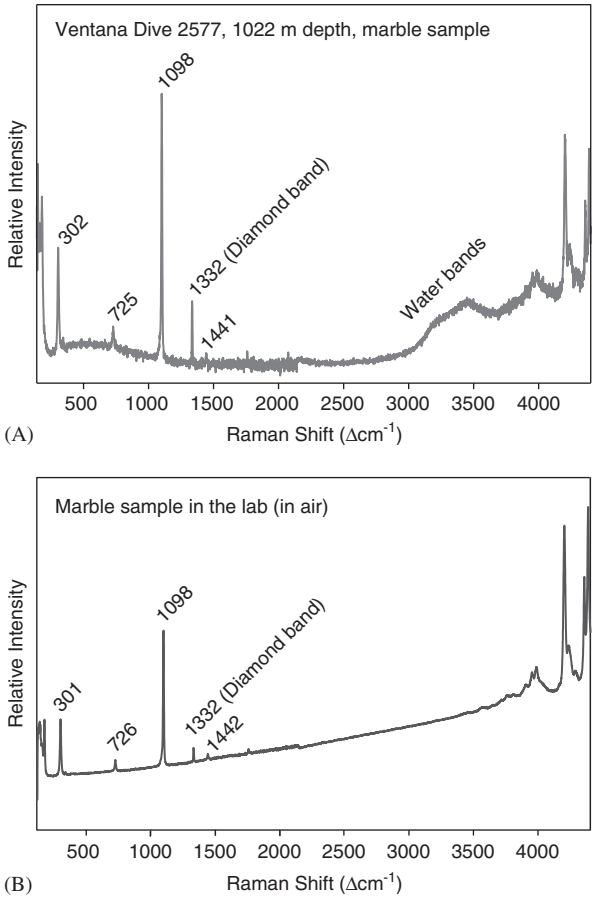

Fig. 13. Spectrum of marble sample (A) on the seafloor at 1022 m depth and (B) in the lab, using PUP to position the focal spot. The immersion optic with a focal depth of 0.15 mm in water was used on the DORISS probe head. Marble is characterized by peaks at ~302, 725, 1098, and 1441 Δ cm^{-1}. The ~1332 Δ cm^{-1} band is from a diamond plate in the probe head to provide a calibration reference. The water stretching bands can be seen at longer wavenumbers in the seafloor data. The peaks on the right of the spectrum are due to impurities in the sapphire pressure window of the immersion optic.

Fig. 14. A slab of Rapakivi granite (from J. Pasteris, Washington University) carried to the seafloor for DORISS/PUP testing.

Fig. 15. A 5 × 4 grid in 0.1 mm increments of the granite slab. The location of the data points is shown in the figure on the left. The mineral at each point is shown in the figure on the right. Mineral identification was performed solely by Raman spectroscopy. The minerals identified were quartz (Qtz), albite (Alb) and Microcline (Mic).

mineral. For cases in which two minerals were detected, they were each assigned half an occurrence, regardless of their relative peak intensities, for the calculation of abundance, as done by Haskin et al. (1997). The chemical composition determined by the Raman point-counting analysis is similar to the average granite composition (Table 2). While granite is not expected to be a target for deep-sea Raman work, this test case provides an example of how DORISS, with the positioning capabilities provided by PUP, can be used to determine bulk rock compositions.

We also attempted to collect spectra from natural targets in the deep ocean. Using PUP we were able to collect a Raman spectrum from a piece of shell (Fig. 17) located at the base of Invert Cliff in Monterey Bay (1024 m depth). In the spectrum we

Table 1
Point-counting data from a granite sample (3 × 3, 5 mm increment grid)

Mineral	% of Grid (%)	Single	Mixed	Point number	
		(*N*)	(*N*)	Single	Mixed
Quartz (SiO_2)	39	2	3	2, 5	1, 7, 9
Albite ($NaAlSi_3O_8$)	28	2	1	4, 6	1
Microcline ($KAlSi_3O_8$)	28	2	1	3, 8	9

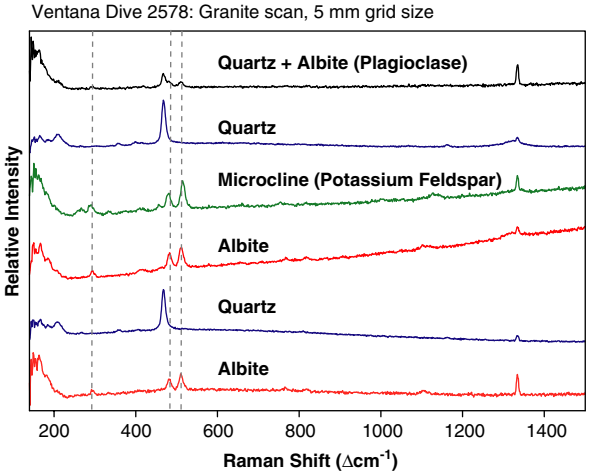

Fig. 16. Spectra of the granite sample on the seafloor at 1022 m depth using PUP to position the DORISS focal spot. These spectra were collected in a grid pattern with 5 mm spacing. The primary mineral components can be seen to be quartz and feldspar: albite (plagioclase feldspar) and microcline (potassium feldspar). The peaks at 1332 Δcm^{-1} are from the diamond calibration reference. The dashed lines indicate the primary albite bands ~290, 479, and 507 Δcm^{-1}.

observe the 1086 Δcm^{-1} peak of calcium carbonate. By looking at the weaker bands present in the lower wavenumber region we were able to determine that calcite and aragonite (polymorphs of $CaCO_3$) are both present. Although these two minerals have the same chemical composition, their structure is slightly different which results in distinct Raman peaks. Calcite exhibits minor peaks at ~281 and ~711 Δcm^{-1}, while the aragonite minor peaks are located at ~206 and ~705 Δcm^{-1} (Urmos et al., 1991).

Some spectra of natural targets were obtained serendipitously. While acquiring spectra from the granite sample on the seafloor, a marine snail climbed onto the sample and approached the laser beam. Because the immersion optic was ~1 mm from the granite sample, the snail could not move

Table 2
Major chemical components of granite

Oxide	From Raman data of granite sample	Average granite composition[a]
	Weight %	Weight %
SiO_2	63.6	70.18
Al_2O_3	9.0	14.47
K_2O	4.5	4.11
Na_2O	4.5	3.48

[a]From Clark (1966).

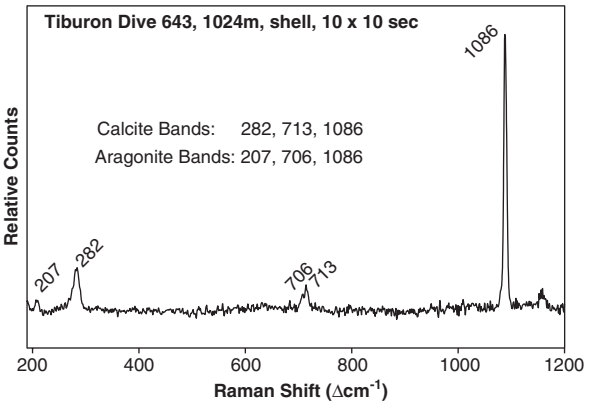

Fig. 17. Spectrum of a shell fragment found on the seafloor at 1022 m depth. The DORISS probe head was positioned using PUP. From the Raman spectrum one can observe that calcite and aragonite (polymorphs of $CaCO_3$) are both present.

fully into the laser path. However, in those spectra we were able to detect carotenoids, which we believe come from the snail shell (Fig. 18). Carotenoids produce strong resonance Raman bands that have been previously observed in Raman spectra of snail shells and corals (e.g., Urmos et al., 1991; Withnall et al., 2003).

Operations were also carried out in Monterey Bay to test the ability of DORISS/PUP to collect in situ

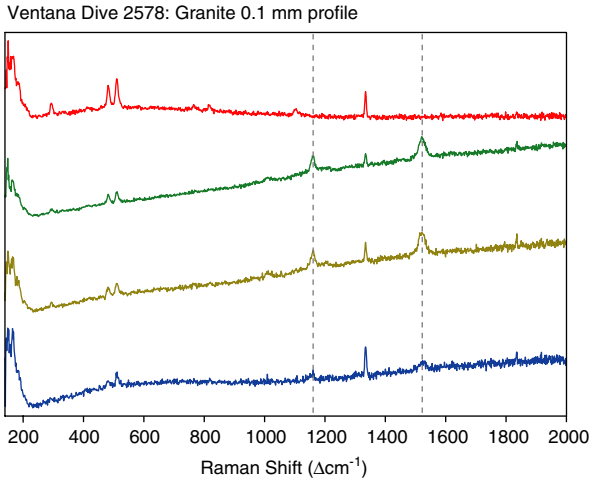

Fig. 18. Spectra from a 0.1 mm profile of granite. All of the spectra are of the mineral albite (plagioclase feldspar). The bottom three spectra show peaks at ~1159 and 1524 Δ cm^{-1} (dashed lines) which are indicative of the carotenoid beta-carotene. The carotenoid appears to come from the shell of a snail that came close to the beam during our acquisitions.

Raman spectra of gas hydrates in preparation for an expedition to Hydrate Ridge, Oregon. Synthetic hydrates were created in a sample cell from a methane–ethane gas mixture at a depth of 1022 m. In this case, the DORISS probe head was mounted horizontally such that the θ axis was used for focusing. PUP was successfully able to focus the laser spot onto the hydrate such that quality Raman data could be obtained (Hester et al., in press).

7. Conclusions

Laser Raman spectroscopy is a valuable geochemical tool for performing in situ analyses of a variety of targets in the deep ocean. The DORISS instrument has already been shown to be effective in analyzing transparent and semi-transparent targets. The PUP greatly enhances the DORISS instrument by allowing it to obtain in situ Raman spectra of opaque targets as well. PUP provides the ability to move in sub-millimeter increments and to scan over the surface of a target in order to perform analyses on the scale of mineral grains. This capability is unique and will lead to new analyses that will further our understanding of various environments in the deep ocean such as natural gas vents, hydrothermal venting sites, geologic formations, hydrate studies, and microbial communities. While PUP was developed for the DORISS instrument, it is capable of being used for any deep ocean sensor with similar positioning requirements.

Acknowledgements

We thank the officers and crews of the R/V *Point Lobos* and R/V *Western Flyer*, and the ROV teams of *Ventana* and *Tiburon*, for their skill and support at sea; collaborator John Freeman of Washington University, St. Louis; Jill Pasteris of Washington University, St. Louis for use of the granite sample; the technical support of John Ferreira, Jim Scholfield, Randy Pricket, Duane Thompson, Tom Marion, and Jose Rosal; and the comments of the editor and three anonymous reviewers. Funding was provided by a grant to MBARI from the David and Lucile Packard Foundation.

Appendix A. Functional requirements

Functional requirements were developed to specify the features needed in a PUP. These include general requirements on how the system will be used and specific performance requirements (Table 3). The performance requirements were based on the operational needs of the DORISS system (i.e., motion and stability requirements) and the operations and limitations of MBARI's two ROVs—ROV *Tiburon* and ROV *Ventana* (i.e., physical size, electrical, and environmental requirements).

A.1. General requirements

1. Shall be capable of operating in stand-alone mode (in air or water) for in-lab use and testing
2. Shall be deployed on the seafloor by an ROV
   - 2.1. Shall be powered by the ROV
   - 2.2. Shall accommodate the DORISS stand-off distance of 5 m
3. Shall maintain stability over full range of motion
   - 3.1. Shall accommodate uneven ocean floor (e.g., slopes up to 30°)
   - 3.2. Shall accommodate a variety of seafloor surfaces (e.g., rocks, sediment, mud)
4. Shall accommodate a sensor head in either the horizontal or vertical orientation
   - 4.1. May be capable of changing orientation during deployment
5. Shall be capable of positioning the laser beam normal to some optimal plane associated with the target

Table 3
Performance requirements

Requirements	Specified value
Motion requirements (for each dimension)	
Minimum position travel of the beam spot	15 cm
Maximum travel increment of the beam spot	0.1 mm
Maximum time to travel full range	1 min
Relative accuracy	1 mm
Pan and tilt range (horizontal or vertical orientation)	$\pm 45^{\circ}$
Physical size requirements	
Maximum sensor weight (in air)	30 kg
Maximum sensor size allowed on mounting surface	$60 \times 20 \times 20$ cm
Maximum weight of complete system (in air)	100 kg
Maximum stowed size (W × H × D)	122 cm × 61 cm × 61 cm
Electrical requirements	
Input power	240 VDC or 110 VAC
Environmental requirements	
Operating depth limit	4000 m
Operating temperature (ambient)	0–50 °C
Operating current (water velocity)	0–0.5 knots

6. Shall have one external camera mounted to the sensor mount for positioning
   6.1. Shall have external lighting
   6.2. Shall have two crossing lasers for positioning reference to assist the pilots in placing the positioner in the appropriate location
7. Shall be controlled by a shipboard scientist
   7.1. Shall have user interface software capable of control and display
   7.2. Shall have position feedback
   7.3. Shall have dual speed positioning
8. May accommodate other (non-DORISS) sensors.

References

Ballard, R., Bryan, W.B., Heirtzler, J.R., Keller, G., Moore, J.G., van Andel, T.H., 1975. Manned submersible observation in the FAMOUS area: Mid-Atlantic Ridge. Science 190 (4210), 103–108.

Brewer, P.G., Malby, G.E., Pasteris, J.D., White, S.N., Peltzer, E.T., Wopenka, B., Freeman, J., Brown, M.O., 2004. Development of a laser Raman spectrometer for deep-ocean science. Deep-Sea Research I 51.

Clark, S.P., 1966. Composition of rocks. In: Clark, S.P. (Ed.), Handbook of Physical Constants. The Geological Society of America, New York, pp. 1–5.

Cline, D., O'Reilly, T.C., Meese, T., Roman, B., Edgington, D. R., 2001. The Environmental Sample Processor (ESP) software design: software for detection and quantification of microorganisms. In: IEEE/MTS Oceans 2001, Honolulu, HI, pp. 287–294.

Haskin, L.A., Wang, A., Rockow, K.M., Jolliff, B.L., Korotev, R.L., Viskupic, K.M., 1997. Raman spectroscopy for mineral identification and quantification for in situ planetary surface analysis: a point count method. Journal of Geophysical Research 102 (E8), 19293–19306.

Hester, K.C., White, S.N., Peltzer, E.T., Brewer, P.G., Sloan, E.D., in press, Raman spectroscopic measurements of synthetic gas hydrates in the ocean. Marine Chemistry

Nakamoto, K., 1997. Infrared and Raman Spectra of Inorganic and Coordination Compounds: Part A. Wiley, New York, NY 387p.

Owen, H., Battery, D.E., Pelletier, M.J., Slater, J., 1998. New spectroscopic instrument based on volume holographic optical elements. Proceedings of the SPIE 2406, 260–267.

Pasteris, J.D., Wopenka, B., Freeman, J.J., Brewer, P.G., White, S.N., Peltzer, E.T., Malby, G.E., 2004. Raman spectroscopy in the deep ocean: successes and challenges. Applied Spectroscopy 58 (7), 195A–208A.

Urmos, J., Sharma, S.K., Mackenzie, F.T., 1991. Characterization of some biogenic carbonates with Raman spectroscopy. American Mineralogist 76, 641–646.

White, S.N., Brewer, P.G., Peltzer, E.T., in press, Determination of gas bubble fractionation rates in the deep ocean by laser Raman spectroscopy. Marine Chemistry

White, S.N., Brewer, P.G., Peltzer, E.T., Kirkwood, W.J., Pasteris, J.D., Nakayama, N., 2003. First expeditionary deployments of the Deep Ocean Raman in situ spectrometer: Eos Trans. AGU, 84(46), Fall Meet. Suppl., Abstract OS32A-0235.

Withnall, R., Chowdhry, B.Z., Silver, J., Edwards, H.G.M., de Olivera, L.F.C., 2003. Raman spectra of carotenoids in natural products. Spectrochimica Acta A 59, 2207–2212.